

Contribution of spatial techniques to the identification of discontinuous basement aquifers in semi-arid zones: the case of the Precambrian basement of Damagaram-Mounio (Centre-East-Niger)

Abstract:

The study area, the Damagaram basement, located in the central south of the Zinder region, has a discontinuous aquifer characterized by a very high failure rate of hydraulic structures (wells and boreholes) and a very low flow rate. In order to improve knowledge of these aquifers and provide access to drinking water for the population of this area, satellite imagery (landsat and aeromagnetic) and field measurement data were used to map fractures. Several techniques, including spatial and directional filtering, were applied to these satellite images to identify, extract and classify the lineaments. The results were validated by previous work and outcrop measurements. Analysis of the spatial distribution shows fractures in the directions N20°-30°; N30°-40°; N40°-50°; N50°-60°; N60°-70°; N70°-80°; N90°-100°; N100°-110°; N110°-120°; N120°-130°; N130°-140°; N140°-150°; N150°-160°; N160°-170° with varying numbers and cumulative lengths. Thus, five major fracture families characterized by directions that are : N40°-60°; N140°.

Keywords : Fractured aquifers, Remote sensing, Damagaram, Basement, Zinder.

1. Introduction :

The crystalline and crystallophyllous basement formations are originally non-aquiferous, as they are characterized by rocks with almost zero permeability. However, they can only become aquifers when they are fractured and/or transformed into alterites, thus becoming discontinuous basement aquifers. In the study area, these aquifers are essentially made up of crystalline and crystallophyll formations, and water only exists in fractures and fissures. In

Commented [L1]: The introduction is very brief. It would be better to enhance it by presenting the results of other studies in this field.

outcrops, water can only infiltrate the granitic arenas of the basins. The decomposition products of these rocks may be permeable, but they are very often clayey, which makes this type of aquifer more complex. Flow rates are very low, never exceeding 0.5 to 5 m³/h, with very high drawdowns. Although the fine sands that cover them are highly favorable to infiltration, these formations are poorly supplied. The success rate of these structures is around 50%, but can fall to less than 25% in young granites and on the slopes of some hills [1]. The study of these types of aquifers requires the identification of zones capable of storing and promoting the circulation of water in these environments. There is therefore an urgent need to develop effective tools for locating drilling sites with a high probability of success [2]. Several prospecting techniques are used to identify areas suitable for drilling, including lineament searches based on spatial imagery. This allows us to locate geological structures (faults, fissures) likely to be responsible for the circulation and storage of groundwater. This technique has been used in the West African basement since the 1980s [3] [4] [5] [6] in [2] and has helped reduce drilling failure rates [7] [8] [9] [10] [11] [12] [13] in [2].

Commented [L2]: Extra spaces between words should be removed

Commented [L3]: Bold ???

The present work is part of this perspective, with the main objective of identifying and characterizing fissured aquifers to improve drinking water supply rates for the populations of the study area.

2. Materiel and methods

2.1. Presentation of the study area

The study area is located in the south-central part of the Zinder region. It covers a large part of the communes of Mazamni, Kassama, Gamou, Moa, Damagaram Takaya and Albarkaram. It lies precisely between 13°52'58" and 14°22'01" North latitude and between 9°08'13" and 10°26'24" East longitude (fig.1). It covers an area of 40,642.4 Km² with a population of 128,000 and a density of 150 hbts/Km² in 2012 [14]. Applying an annual growth rate of 4.7%, the population of this area in 2023 is estimated at around 200,000. Agriculture is the population's main activity, followed by livestock breeding.

Commented [L4]: Reference???

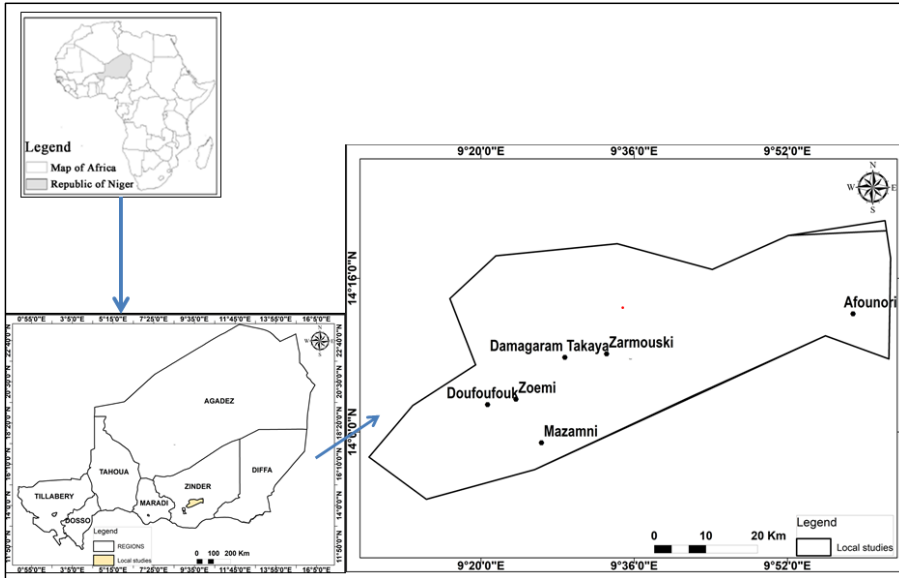


Figure 1 : Location of study area [In the continent of Africa and the country of Nigeria](#)

Commented [L5]: -Some of the texts in Figure 1 are not readable.
-The map scale does not correspond with the area (40,642.4 Km²). Please check it.

Formatted: English (United States)

2.2. Geology and hydrogeology of study area

From a geological point of view, the study area lies on the Precambrian formations of the Damagaram basement (fig.2). These plutonic and metamorphic formations are mainly formed by hyperalkaline granites, quartzites and calcium silicate gneisses.

These crystalline and crystallophyllous basement formations are Tuareg and Benin-Nigeria shield appendages remobilized during the Pan-African orogeny and cratonized since 500 ± 100 Ma [15]. Subsequently, intraplate magmatism of the alkaline type affected the Damagaram basement between 320 and 290 Ma. Oriented East-West, these two basement units culminate at an altitude of 600 m and are shaped like a horseshoe with a width of around 130 km [16].

The petrographic characteristics and emplacement conditions of the Damagaram basement geological units enable us to distinguish two (2) major groups: metamorphic and granitic formations.

➤ Metamorphic formations

The Damagaram basement is made up of metamorphic formations attributed to the Precambrian period and comprises 2 sub-groups in the area:

- **calcium-silicate gneisses**, locally hornfels-facies and greenish-gray in color, with a dense network of fissures at the surface. The main constituent minerals are feldspars, a few plagioclase minerals, tourmaline and epidote;
- **Quartzites**, gray to white in color, form the relief of the region, are highly folded and affected by detachments. The minerals are mainly quartz, with muscovite, tourmaline and iron oxides;
- **Damagaram-Mounio intrusive rocks**

The folded series are crossed by intrusive granites [17], distinguishes two subgroups:

- **ancient granites**, comprising two types of granite: porphyritic calc-alkaline granites, heterogeneous in texture and whose main minerals are quartz, microcline, plagioclase, blue-green amphibole and biotite; 2-mica granites and biotite granites, considered tectonic, occur in the form of small, widely scattered massifs. Pink in color, these granites have a grainy texture and a mineralogical composition that includes quartz in clusters, fissured microcline, oligoclase and sometimes muscovite.
- **Younger granites, on the other hand**, are anorogenic, organized in annular structures in the form of small scattered masses. In the Mazamni area, riekkite granites are the most common. Its color is very light to bluish-gray, the texture is grainy and the main constituent minerals are exomorphic to sub-automorphic quartz aggregates, fissured potassium feldspars and prismatic riekkite;

Hydrogeologically, the discontinuous basement aquifer is the main aquifer tapped by wells and boreholes in the study area (fig. 2). This aquifer is essentially made up of crystalline and crystallophyll formations, with water existing only in the fractures and fissures of the latter. In outcrops, water can only infiltrate the granitic arenas of the basins. Granite decomposition products may be permeable, but they are very often clayey, which makes this type of aquifer more complex. Flow rates are very low, never exceeding 0.5 to 5 m³/h, with very high drawdowns. Although the fine sands that cover them are highly favorable to infiltration, these formations are poorly supplied. The success rate of these structures is around 50%, but can fall to less than 25% in young granites and on the slopes of some hills [1]. Water inflows are obtained between 10 and 80 m. In exceptional cases, they reach 100 m. The average depth of the structures is 80 m, with about 20 m of overburden.

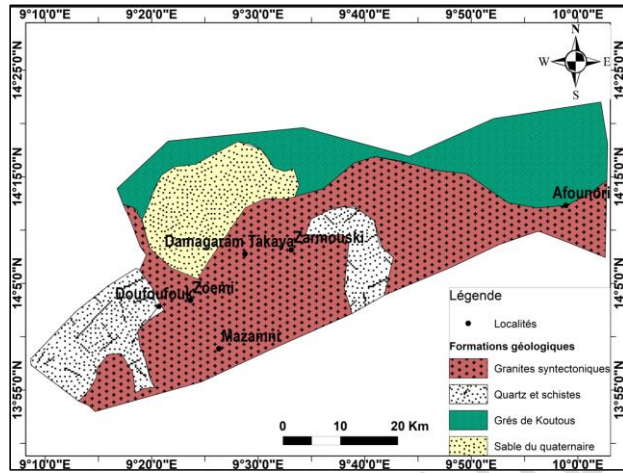


Figure 2: Geology of the study area

Commented [L6]: The legend of the map should be written in English.

2.3. Data and materials

The data used in this study include the aeromagnetic image (scene, acquired on Columns and Rows: 4160, 2416); the Digital Terrain Model (DEM, MNT, 30m resolution); the 1/500000-scale geological map of Niger and the topographical map of the Zinder region.

The field data concern measurements of the direction and dip of geological structures.

These images were processed and interpreted using ENVI 4.3, ArcGis 10.3, Linwin and Excel.

Digital Elevation Model (DEM, 30 m resolution, scenes: 17-008 and 17-009, NASA, USGS/2014)

2.4. Processing

2.4.1. Pre-processing

These are preliminary operations applied to the images to make them more legible and superimposable. They mainly concern geometric and radiometric corrections. Geometric corrections involve rectifying satellite images so that they can be superimposed on other images or reference cartographic documents [18]. To do this, the first phase involves superimposing the image with a reference cartographic document using landmarks. As for

radiometric correction, this deals with the effects of the various artifacts that disrupt radiometric measurement, notably sensor defects and atmospheric haze that alter images [18].

2.4.2. Sobel directional filter

One of the aims of filtering is to clean up the signal, eliminating as much noise as possible while preserving as much information as possible [19]. Sobel's directional filter was used in this work. It enables structural and lithological discontinuities to be accentuated for better lineament discrimination [2] [20]. This filter enables lineaments to be detected in all directions. For this work, Sobel's 7x7 matrix directional filters (fig. 3) with orientations N-S, E-W, NE-SW, NW-SE are used. This matrix has given satisfactory results in the work of several authors [2] [20] [21] [22] [23].

Formatted: Font: Not Bold

N-S						
1	1	1	2	1	1	1
1	1	2	3	2	1	1
1	2	3	4	3	2	1
0	0	0	0	0	0	0
-1	-2	-3	-4	-3	-2	-1
-1	-1	-2	-3	-2	-1	-1
-1	-1	-1	-2	-1	-1	-1

E-O						
-1	-1	-1	0	1	1	1
-1	-1	-2	0	2	1	1
-1	-2	-3	0	3	2	1
-2	-3	-4	0	4	3	2
-1	-2	-3	0	3	2	1
-1	-1	-2	0	2	1	1
-1	-1	-1	0	1	1	1

NE-SO						
0	1	1	1	1	1	2
-1	0	2	2	2	3	1
-1	-2	0	3	4	2	1
-1	-2	-3	0	3	2	1
-1	-2	-4	-3	0	2	1
-1	-3	-2	-2	-2	0	1
-2	-1	-1	-1	-1	-1	0

NO-SE						
2	1	1	1	1	1	0
1	3	2	2	2	0	-1
1	2	4	3	0	-2	-1
1	2	3	0	-3	-2	-1
1	2	0	-3	-4	-2	-1
1	0	-2	-2	-2	-3	-1
0	-1	-1	-1	-1	-1	-2

Figure 3: 7x7 matrix of Sobel directional filters

2.4.3. Manual lineament extraction using visual analysis

Manual lineament extraction is an excellent approach that has been used by several authors ([2] [20] [21] [23] [24]). It consists in manually extracting image lineaments from visual observation by photo-interpretation (fig. 4). This operation calls on the observation and reasoning skills of the photo-interpreter, but also requires a good knowledge of the area for an objective and realistic sorting of the phenomena sought (structural lineaments) [2] [24]. The

segments (lineaments) are traced directly on the screen, with localized magnification for structures that are difficult to observe.

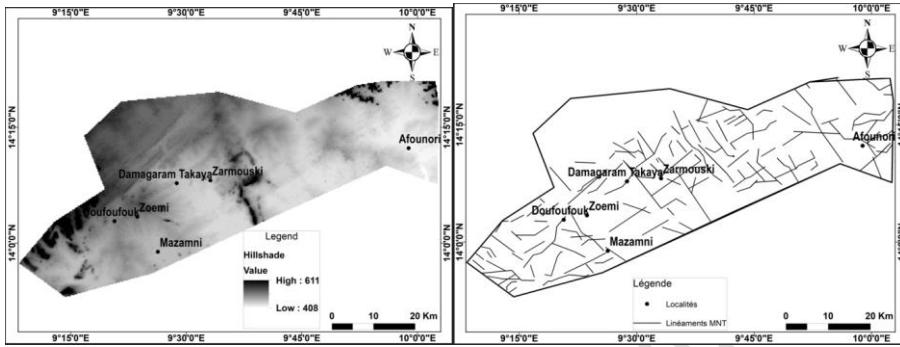


Figure 4 : (left) Hillshad image; (right) Manual extraction of lineaments.

3. Results and discussion

3.1. Results

3.1.1. Lineament mapping

The results of manual lineament extraction from aeromagnetic and DTM images are shown in the figure. These lineaments vary greatly in direction and size on all images. As a result, the spatial distribution of lineaments in terms of number and cumulative length is not homogeneous.

3.1.2. Directional distribution of aeromagnetic image lineaments

Figure 5 shows the directional rosette and the frequency of fracture directions obtained after statistical processing. 68 geological fractures are highlighted (fig. 6 left). These figures show that fracture directions $N120^{\circ}\text{-}140^{\circ}$; $N100^{\circ}\text{-}120^{\circ}$; $N40^{\circ}\text{-}60^{\circ}$; $N140^{\circ}\text{-}160^{\circ}$ are predominant (fig. 6 right). Indeed, the percentages in number of these fractures are respectively 36% ($N120^{\circ}\text{-}140^{\circ}$), 21% ($N100^{\circ}\text{-}120^{\circ}$), 14% ($N40^{\circ}\text{-}60^{\circ}$) and 13% ($N140^{\circ}\text{-}160^{\circ}$). The percentage of fractures in cumulative length is 42% ($N120^{\circ}\text{-}140^{\circ}$), 13% ($N100^{\circ}\text{-}120^{\circ}$), 14% ($N40^{\circ}\text{-}60^{\circ}$) and 18% ($N140^{\circ}\text{-}160^{\circ}$) respectively.

Commented [L7]: The figure number should be introduced.

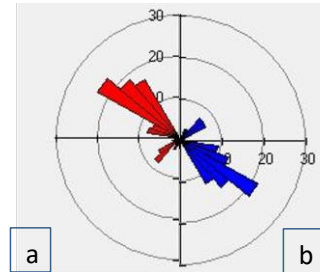


Figure 5: Directional fracture pattern: cumulative length (a) and number (b)

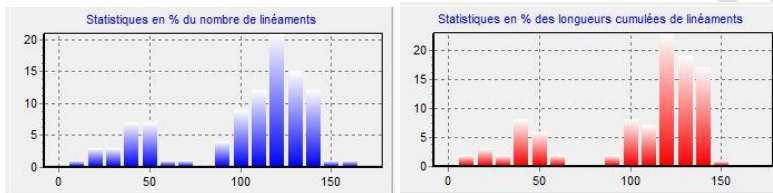


Figure 6: Directional diagram showing the frequency of DTM fractures: cumulative length (left) and number (right)

3.1.3. Directional distribution of DTM lineaments

Figures 7 and 8 show the rosette and directional diagram showing the direction and frequency of DTM fractures in terms of cumulative length and number. There are 227 fractures resulting from this processing, more than those obtained from aeromagnetic image processing (Fig. 8a). Five major fracture families can be identified, each characterized by its own direction: N40°-60°; N140°-160°; N120°-140°; N60°-80°; N80°-100°, represented respectively by 19%; 18%; 17%; 13% and 13% of the total number of fractures (fig. 8b). From these directions stand out the more restricted directions N50°-60°, N140°-150°, N130°-140° with respectively 12%, 11% and 10% of the total. In terms of cumulative length, these five major fracture families (N40°-60°; N140°-160°; N120°-140°; N60°-80°; N80°-100°) are the most represented, with cumulative lengths of 22%, 22%, 19%, 11% and 11% respectively.

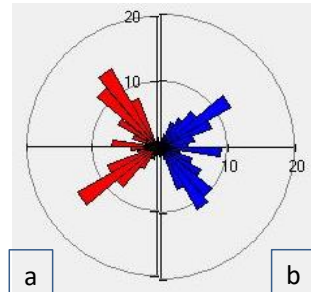


Figure 7: Directional fracture pattern: cumulative length (a) and number (b).

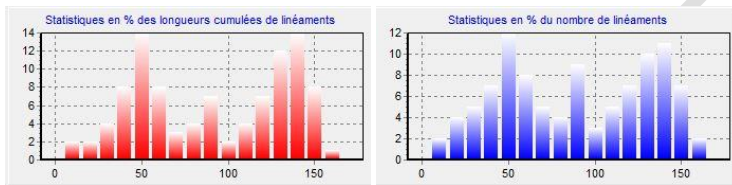


Figure 8: Directional diagram showing fracture frequency from DTM: cumulative length (left) and number (right)

3.1.4. Correlation between major fractures and the two types of lineaments

Superimposing the lineament maps on the major fractures derived from the geological map shows a good correlation between the two (fig. 9). Highlighting these fractures is important for lineament validation, even if they represent less than 5% of all major lineaments mapped [25]. This is because the fractures identified on the geological map are genuine geological discontinuities validated by field observations. Moreover, this superposition also reveals multi-kilometre lineaments (especially those in the aeromagnetic image) that exceed the faults shown on the geological map, and which may have a regional impact. On the other hand, the density of lineaments is greater than that of geological faults (especially those in the DTM image). Furthermore, the N40°-60° and N140°-160° directions are still the most common for these three types of geological structure.

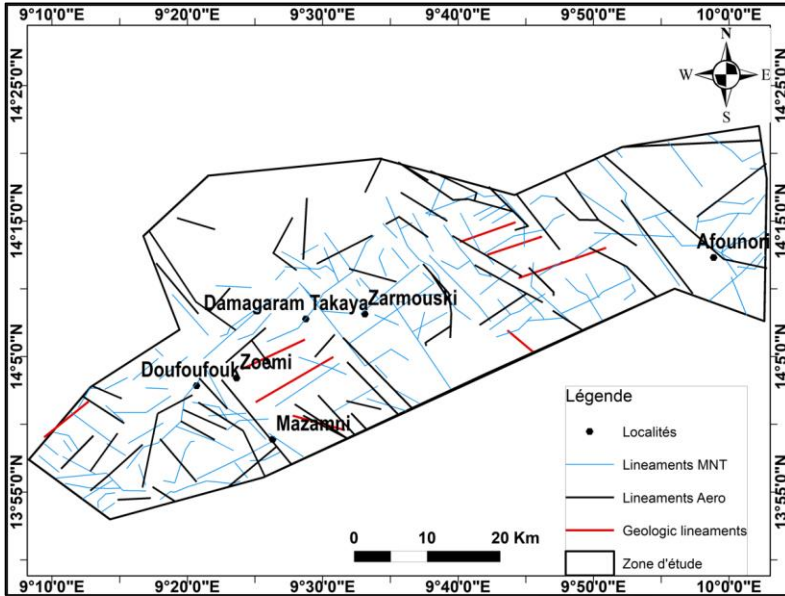


Figure 9: Superposition of lineaments with regional tectonic structures

Commented [L8]: The legend of the map should be written in English.

3.2. Discussions

The mapping study of the lineaments using DTM and aeromagnetic images highlighted the types, intensities, directions and cumulative lengths of these geological structures in the study area. Complemented by field measurements, this study contributes to the identification of fractured aquifers on the one hand, and significantly to the improvement of knowledge of the latter on the other. The use of DTM and aeromagnetic images has produced satisfactory results in basement fracturing studies worldwide [10][2] [20] [21] [26].

In the Damagaram basement, among the fracture classes observed from aeromagnetic imagery, DTM and geological map, two main directions $N140^{\circ}-160^{\circ}$ and $N40^{\circ}-60^{\circ}$ stand out from the others in terms of percentage of number and cumulative fracture lengths. These two directions highlight the regional Liberian accidents (NW-SE) and the NE-SW directions of the major shear corridors [2]. These results are in good agreement with those noted by several works on the West African basement in general [3] [10] [25] and the Niger basement zones in particular [2] [20] [26]. These directions should be sought for future drilling, as according to [10] in [2], the success rate increases with the length of the lineament, especially in granitic

formations. Field measurements have revealed several types of vein (quartz; pegmatites...), with biotite tension cracks in various directions (fig. 10). Once altered, these veins constitute preferential zones for groundwater infiltration and circulation [2]. Also, fractures, veins and faults that are late, opening or extending may have higher hydraulic conductivity and permeability than the initial crystalline rock. These zones are potential targets for drilling during geophysical prospecting. The work of [4] in the West African basement demonstrated the influence of vein-bearing rocks on the success and high productivity of boreholes drilled in birimian shales [2].

According to [27], these two directions are particularly well represented throughout the massif: 50° to 60° and 150° . They are orthogonal, and the accidents belonging to them appear to be contemporaneous, with a slight anteriority of early operation for those in the 50° - 60° direction. Both represent shear directions whose effects are clearly observable, with a system of conjugate detachments (dexter E-W and sinister ENE-WSW) [22] of the micashist and quartzite formation of the order of 5 km at most, along the horizontal plane. Both of these accident families are frequently accompanied by vein fillings of brecciated quartz, with or without silicified breccia. Quartzites are frequently parallel to these fractures, or are largely rolled back at their contact.

Two other fracture directions can be seen, complementary to the previous ones: 20° - 30° and 90° - 100° , representing extension and compression fractures, which have only rarely given rise to significant rejections. They are often accompanied by massive quartz fillings, sometimes geodic (the 90° - 100° direction, perpendicular to the mean direction of the series and to the directions of the soft tectonics, represents the direction of compression).

The 50° - 60° accidents seem to have had a permanent effect thereafter. The southern edge of the Zinder Massif also appears to correspond to one of these ancient accidents, locally underlined by a filling of pegmatoids and young rhyolites. Lastly, this accident direction conditions the entire current distribution of cover on the basement, probably linked both to the distribution of deposits in zones of varying depth (existence of gravel filled by Koutous sandstones) and to that of erosion zones, oriented by the existence of fractures and the presence of ripples due to their operation.



Figure 10: Tectonic structures observed on outcrops in the study area.

4. Conclusion

Landsat and aeromagnetic satellite images have been processed to produce lineament maps (faults and fissures) of the study area. The results, validated by previous work and outcrop measurements, show fractures of widely varying directions and lengths. However, we can distinguish five major families of predominant fractures characterized by directions $N40^{\circ}-60^{\circ}$; $N140^{\circ}-160^{\circ}$; $N120^{\circ}-140^{\circ}$; $N60^{\circ}-80^{\circ}$; $N80^{\circ}-100^{\circ}$, represented respectively by 19%; 18%; 17%; 13% and 13% of the total number of fractures, i.e. 80% of the total. These directions highlight the regional Liberian accidents (NW-SE) and the NE-SW directions of the major shear corridors. These directions should be sought for future drilling. In addition, lineament studies are not sufficient on their own, as they represent a small-scale approach. Localized geophysical studies will therefore be required to confirm the hypotheses put forward by this lineament structure study.

Conflicts of Interest

The authors declare no conflicts of interest regarding the publication of this paper.

References

- [1] Zinder Regional Directorate of Hydraulics and Sanitation (2008) Monograph of the Zinder region, Report, 2008.
- [2] Maman Sani Abdou Babaye, Illias Alhassane, Issa Malam Salmanou S, Issoufou Boukari Ousmane, Moussa Konate, 2021: Synergistic approach between spatial technique and field data for the identification of fissured basement aquifers in a semi-arid environment (Liptako, South-West Niger). Bulletin of the Scientific Institute, Rabat, Earth Sciences Section, 2021, n°43, 53–68. e-ISSN: 2458-7184.
- [3] Engalenc M. 1978. Method for the study and research of groundwater in crystalline rocks of West Africa. Inter-African Committee for Hydraulic Studies (CIEH)-Geohydraulics, 318 p.
- [4] Engalenc M. 1981. Method of study and research of groundwater in crystalline rocks-Atlas of photo-interpretation. Inter-African Committee for Hydraulic Studies (CIEH)-Geohydraulics, Volume III. 38p.
- [5] Guiraud R. & Travi Y. 1990. Synthesis of knowledge of the hydrogeology of West Africa. Crystalline and crystallophyllian basement and ancient sedimentary. Avignon University CEFIGRE, 2nd Ed., 147 p.
- [6] Corgne S., Magagi R., Yergeau M. et al. 2010. An integrated approach to hydro-geological lineament mapping of a semi-arid region of West Africa using Radarsat-1 and GIS. Remote Sensing of Environment, 114(9), 1863–1875.

[7] Savadogo A.N. 1984 Geology and hydrogeology of the crystalline basement of Upper Volta-Regional study of the Sissili watershed. State Doctoral Thesis, University of Grenoble 1, 350 p.

[8] Faillat J.P. 1986. Fissured aquifers in humid tropical zones: structure, hydrodynamics and hydrochemistry (West Africa). Doctoral Thesis, University of Sciences and Technology Languedoc, Montpellier, 480 p.

[9] Biemi J. 1992. Contribution to the geological, hydrogeological and remote sensing study of sub-Saharan watersheds of the Precambrian basement of West Africa: hydrostructural, hydrodynamic, hydrochemistry and isotopy of discontinuous aquifers of furrows and granitic areas of the upper Marahoué (Côte d'Ivoire). National Doctoral Thesis, University of Abidjan, Côte d'Ivoire, 493p.

[10] Koussoubé Y. 1996 Hydrogeology in the crystalline basement environment of Burkina Faso. Case of the Bidi lowland watershed (Yatenga province). Third cycle Doctoral Thesis, Cheikh Anta Diop University, 210 p.

[11] Savané I. 1997 Contribution to the geological and hydrogeological study of discontinuous aquifers of the crystalline basement of Odiénné (North-West of Ivory Coast). Contribution of remote sensing and a hydrogeological information system with spatial reference. Doctoral thesis, University of Cocody (Abidjan), 396 p.

[12] Edet A.E., Okereke C.S., Teme S.C. et al. 1998 Application of remote-sensing data to groundwater exploration: A case study of the Cross River State, southeastern Nigeria. *Hydrogeology Journal*, 6, 394–404.

[13] Kouamé K.F. 1999 Hydrogeology of discontinuous aquifers of the semi-mountainous region of Man-Danané (Western Ivory Coast). Contribution of satellite image data and statistical and fractal methods to the development of a

spatially referenced hydrogeological information system. Third cycle doctoral thesis, University of Cocody (Abidjan), 194 p.

[14] National Institute of Statistics (2013), National census of localities. Report, (2013).

[15] Ousmane B. (1988) Geochemical and isotopic study of the aquifers of the basement of the Sahelian strip of Niger (Liptako, South Maradi and East Zinder), State doctoral thesis, University of Niamey.

[16] ISSOUFOU S. (2013) Hydrodynamic, hydrochemical and isotopic studies of groundwater in the Korama/South Zinder watershed, Niger: Impacts of climate variability and anthropogenic activities. Thesis Univ.Niamey.

[17] GREIGERT J. (1968): Groundwater in the Republic of Niger, BRGM, 68 ABI 006 NIA, 2nd volume 423 pages.

[18] Issa Malam Salmanou S., Issoufou S., Abdou Babaye MS., Boureima O., (2018) Dynamics of land use and the evolution of ponds in the upper Korama watershed, Rural commune of Droum, Zinder region. *Afrique SCIENCE* 14(4) (2018) 346–358.

[19] Maitine Bergounioux (2010): Some filtering methods in image processing. 2010. Hal-00512280v1

[20] Alhassane, I., Sani, A.B.M., Souleymane, I.M.S. and Wagani, I. (2023) Application of Spatial Techniques for the Identification of Discontinuous Aquifers of the Basement in Semi-Arid Environment: A Case of Bagzan Mount Plateau, Air Massif (North, Niger). *Journal of Water Resource and Protection*, 15, 581-596. <https://doi.org/10.4236/jwarp.2023.1511032>

[21]Badamassi, K.M.M. (2021): Petrostructural characterization of Pan-African formations in Damagaram province (South-East Niger). Single doctoral thesis of the Abdou Moumouni University of Niamey, p.124.

[22]LAWALI IDI Chamsi (2024) Petrogenesis and magmatic evolution of felsic anorogenic suites of Tirmini and Badaraka (Damagaram, south-eastern Niger): implications of geochronology and isotopic geochemistry, Single doctoral thesis in geology, Abdou Moumouni University of Niamey, Niger.

[23]Kouamé K.F., Penven M.J., Kouadio B.H. et al. (2006) Contribution of aster de terra images and a digital elevation model to the morphostructural mapping of the Toura massif (western Côte d'Ivoire). *Remote Sensing*, 6(2), 103–121.

[24] Issaka Boubacar Ali, Mahaman Bachir Saley, Vano Mathunaise Sorokoby and Aimé Koudou, (2022) Contribution of remote sensing and GIS to the identification of favorable areas for the installation of hydraulic drilling in the department of Téra, western Niger. *Afrique Science* 20(5) (2022) 75-92. Issn 1813-548x, [Http://Www.Afriquescience.Net](http://www.Afriquescience.Net).

[25]Avy Stéphane. Koffi, Kouassi Eric Germain. Kouakou And Yenipoho Onésiphore. Tuo (2021): Extraction by remote sensing of the major fracture network for groundwater prospecting in the commune of Niakaramandougou, *American Journal Of Innovative Research And Applied Sciences*. Issn 2429-5396 I [Www.American-Jiras.Com](http://www.American-Jiras.Com).

[26]M. Konaté, M. Denis, M. Yahaya and M. Guiraud, (2007) Extensive and Transtensive Structuring in the Devono-Dinantian of the Tim Mersoï Basin (Western Border of the Aïr, Northern Niger). *Annals of the University of Ouagadougou - Series C*, Vol. 005, June 2007;

Koussoubé Y., Savadogo A.N. & Nakolendoussé S. (2003) Different signatures of crystalline basement fractures in the Sahelo-Sudanian zone of Burkina Faso (Bidi watershed, Yatenga province). *Remote Sensing*, 3(5), 419–427.

Koussoubé Y., Savadogo A.N., Nakolendousse S. et al. (2006) Efficiency of three lateral investigation methods in highlighting contacts between geological

formations of the Lower Proterozoic of Burkina Faso. *Journal of Sciences*, 6(2), 105–115.

Lasm T. (2000) Hydrogeology of fractured basement reservoirs: Statistical and geostatistical analyses of fracturing and hydraulic properties. Application to the mountain region of Ivory Coast Archean Domain). Doctoral thesis, University of Poitiers, 272 p.

[27] R. Mignon, 1970: Geological study and prospecting of Damagaram Mounio and South Maradi, BRGM, 1970.

UNDER PEER REVIEW